이학석사 학위논문

$(Sr,K)BiO_3$ Thin Film Growth with Post-annealing Method by using Pulsed Laser Deposition

펄스레이저 증착에서 포스트 어닐링 기법을 이용한

$(Sr,K)BiO_3$ 박막 증착

2022 년 6 월

서울대학교 대학원

물리천문학부

이종화

$(Sr,K)BiO_3$ Thin Film Growth with Post-annealing Method by using Pulsed Laser Deposition

펄스레이저 증착에서 포스트 어닐링 기법을 이용한 $(Sr,K)BiO_3$ 박막 증착

지도교수 노태원

이 논문을 이학석사 학위논문으로 제출함

2022 년 6 월

서울대학교 대학원

물리천문학부 물리학전공

이종화

이종화의 석사 학위논문을 인준함

2022 년 6 월

위 원 장	이규철	(인)
부 위 원 장	노태원	(인)
위 원	장준호	(인)

Abstract

Recently, the growth of perovskite oxide film has attracted a lot of attentions due to its physical property[1]. Among perovskite oxide thin films, there are many studies on $BaBiO_3$ (BBO) to adjust the characteristic of BBO. However, $SrBiO_3$ (SBO) is not attracting attention even though it has similar properties to BBO. There was only one case in which SBO thin films were grown using Molecular Beam Epitaxy (MBE) in 2019[2].

Here, I grew $(Sr,K)BiO_3$ (SKBO) thin films (bulk T_c ~ 12 K) doped with Potassium (K) to SBO. The Oxygen vacancy was reduced using the *in-situ* post-annealing method. Temperature, oxygen pressure, and laser fluence were changed to see different properties of SKBO films. I also controlled the post-annealing conditions to show the importance of the post-annealing method. The properties of SKBO thin films were investigated through X-ray Diffraction, Ellipsometer, and Transport measurements. I grew a new kind of bismuthate film, and it provides a new way to study bismuthate thin films.

Contents

List of Figure

one is data after 168 hours (168 h later). The scan range is from (a) 7° to 107° and (b) 15° to 55°.

Fig. 3-4 X-ray Diffraction 2θ-θ scan with post-annealing method by varying temperature. The laser fluence and oxygen pressure are fixed at 1.1 J/cm^2 and 100 mtorr. The post annealing condition is that temperature is 700℃ Oxygen pressure is 400 torr for 40 minutes. The scan range is from (a) 7° to 107° and (b) 15° to 55°.

Fig. 3-5 X-ray Diffraction 2θ-θ scan with post-annealing method by varying laser fluence. The temperature and oxygen pressure are fixed at 700℃ and 100 mtorr. The post annealing condition is that temperature is 700℃ Oxygen pressure is 400 torr for 40 minutes. The scan range is from (a) 7° to 107° and (b) 15° to 55°.

Fig. 3-6 X-ray Diffraction 2θ-θ scan with post-annealing method by varying oxygen pressure. The laser fluence and temperature are fixed at 0.9 J/cm^2 and 700℃. The post annealing condition is that temperature is 700℃, Oxygen pressure is 400 torr for 40 minutes. The scan range is from (a) 7° to 107° and (b) 15° to 55°

Fig. 3-7 The SKBO/STO samples. Post-annealing temperature and time are varied. Post-annealing oxygen pressure is fixed at 400 torr. All samples have the same films growth condition (T = 700℃, Oxygen pressure = 100 mtorr, Laser fluence = 0.9 J/cm^2)

Fig. 3-8 X-ray Diffraction 2θ-θ scan of changing post-annealing time. The scan range is from (a) 7° to 107° and (b) 18° to 60°

Fig. 3-9 X-ray Diffraction 2θ-θ scan of changing post-annealing temperature. The scan range is from (a) 7° to 107° and (b) 38° to 50°

Fig. 3-10 The Reciprocal Space Mapping (RSM) around the STO (103) peak for a SKBO film. Film growth condition is that T = 700°C, Oxygen pressure = 100 mtorr and Laser fluence = 0.9 J/cm^2. Post-annealing condition is that T = 700°C, Oxygen pressure = 400 torr for 40 minutes.

Fig. 3-11 Ellipsometer data of SKBO films. All samples have the same growth condition (optimized growth condition) except from laser fluence. The laser fluence is varied from 0.5 J/cm^2 to 1.1 J/cm^2.

Fig. 3-12 Ellipsometer data of SKBO films. All samples have the same growth condition (optimized growth condition) except from post-annealing time. The post-annealing time is varied from 40 minutes to 160 minutes.

Fig. 3-13 The transport measurement data of SKBO film. The SKBO films are grown under optimized condition and only changes laser fluence. The laser fluence is (a) 0.9 J/cm^2 and (b) from 0.5 J/cm^2 to 1.1 J/cm^2.

Chapter 1

Introduction

Perovskite Oxide heterostructures have emergent physical properties such as superconducting behavior[1,3] and two-dimensional electronic gas[4]. Recently, many researchers have focused on the interface and junction of oxide heterostructure to create quantum devices[5-9]. In the perovskite oxide heterostructure, the bismuthate heterostructure is attracting attention because it is useful for investigating superconductivity[7]. So, there have been many attempts to grow bismuthate thin films[10-16].

$BaBiO_3$ (BBO) has a perovskite ABO_3 structure. Ba is located on A-site, and Bi and Oxygen are located inside(**Fig. 1-1(a)**). BBO is an interesting material. According to Hund's rule, BBO should show metallic behavior. But in fact, BBO shows insulating behavior. It is a widely known that BBO has Charge Density Wave (CDW) and it makes BBO to show insulating behavior[10,11]. Superconductivity $(Ba,K)BiO_3$ (BKBO) (T_c ~ 30K) and $Ba(Pb,Bi)O_3$ (BPBO) (T_c ~ 12 K) appear when holes are doped into BBO, such as potassium (K) or lead (Pb)[13-15]. There have been attempts to grow BKBO and BPBO thin films. The films of BKBO and BPBO also exhibit superconductivity although the critical temperature is lower[16-23].

However, the BBO family has large lattice constants (a_{BBO} ~ 4.33 Å, a_{BKBO} ~ 4.28 Å, a_{BPBO} ~ 4.30 Å), and these makes large lattice mismatches on commercially available substrates (*e.g.* $SrTiO_3$; a ~ 3.905 Å). To reduce lattice mismatch, it is a good idea to grow other bismuthate films that have similar properties to BBO but have small lattice constants. The $SrBiO_3$ (SBO) family is one of the candidates.

There is $SrBiO_3$ (SBO) (a_{SBO} ~ 4.25 Å) material that have similar properties to BBO. Comparing SBO and BBO, Sr is in A-site instead of Ba(**Fig. 1-1(b)**). SBO also has a CDW and shows insulating behavior[24]. SBO is the parent compound of a high T_c superconductor. $(Sr,K)BiO_3$ (SKBO) is one of the SBO family made of potassium doped into SBO. When the potassium ratio is 0.45 to 0.6, a superconductivity phenomenon occurs, and the critical temperature T_c is almost 12 K in bulk state[25].

In general, the SBO family has a small lattice constant (a_{SBO} ~ 4.25 Å, a_{SKBO} ~ 4.22 Å) than BBO family. So, it can reduce lattice mismatch when growing SBO family on the STO substrate. However, despite these advantages, SBO has not been noticed. Only one case of SBO thin films were grown using Molecular Beam Epitaxy (MBE) in 2019[2], and there is no report on SKBO thin films.

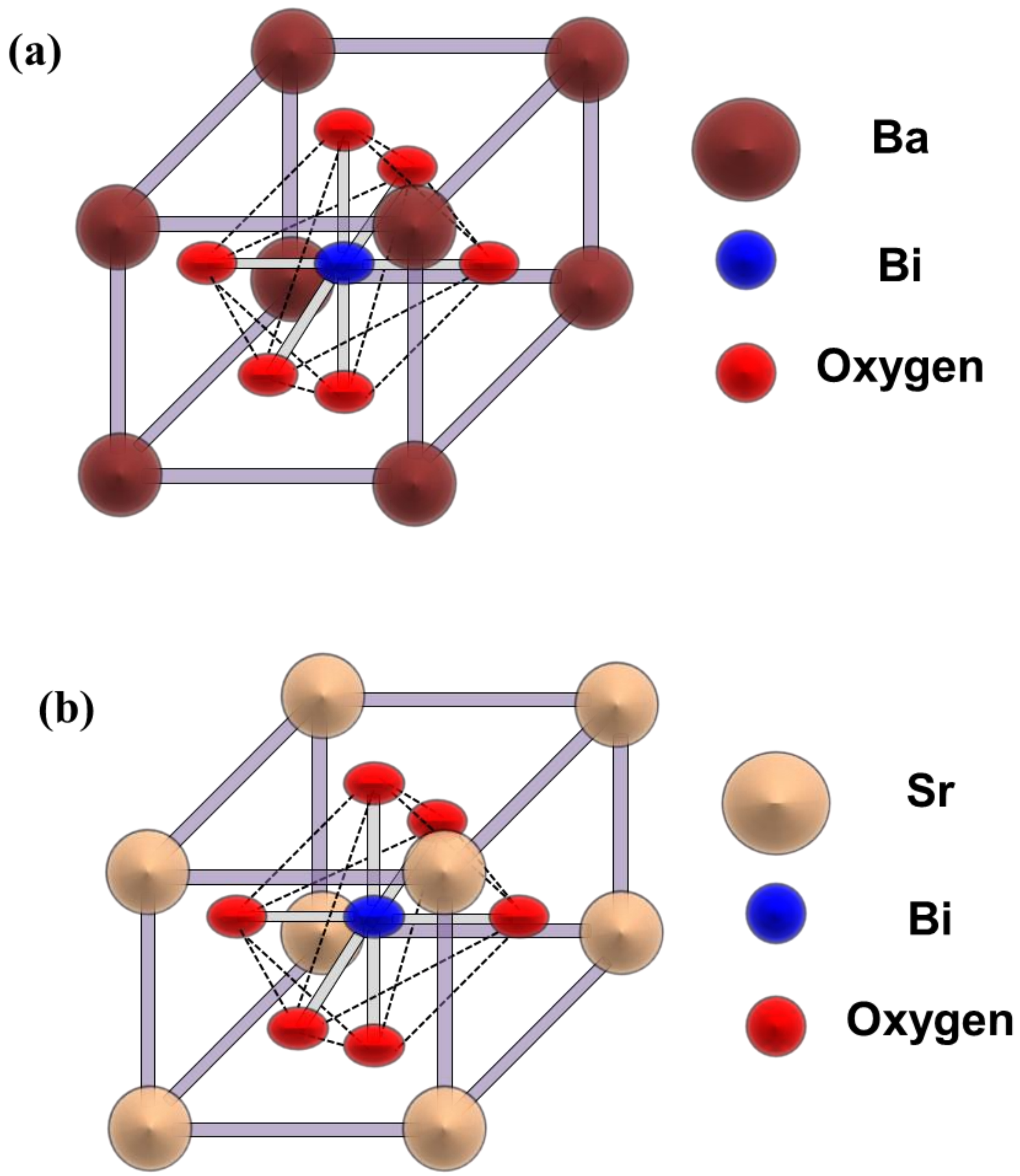

Fig. 1-1 The schematic of perovskite structure (ABO_3). (a) is the schematic of $BaBiO_3$ (BBO) and (b) is the schematic of $SrBiO_3$ (SBO). The difference of BBO and SBO is the atoms which is located at A-site.

I grew SKBO films on $SrTiO_3$ (STO) (001) substrates using Pulsed Laser Deposition (PLD). The growth of SKBO thin films has a problem of oxygen vacancy. BKBO is a similar to SKBO, and the growth of BKBO films has the same problem. In BKBO thin films growth, an *in-situ* post-annealing method was performed to reduce oxygen vacancy[20]. So, I used the same method. When using the *in-situ* post-annealing method, the SKBO thin films grow epitaxially on the STO substrate. After that, I changed the film growth conditions and post-annealing conditions to see how each condition affects the properties of SKBO films. To verify that the SKBO film has epitaxially grown, High resolution X-ray Diffraction (XRD) was used to perform 2θ-θ scans and Reciprocal Space Mapping (RSM) measurements of the SKBO films. To distinguish the optical conductivity of the SKBO, ellipsometer was used. I performed the transport measurement to see the resistance of the SKBO films. From these data, it can be seen that the *in-situ* post-annealing method is important for growing a thin film and affects the properties of the SKBO thin films.

Chapter 2

Experimental Section

2.1 Pulsed Laser Deposition : Growth of (Sr, K)BiO_3 film

SKBO films were grown using $SrTiO_3$ (STO) (001) substrate (Crystec. Germany). Before growing the films, the STO substrate was treated with acid. First, soak the STO substrate in Deionized water (DI water) for 10 seconds. Next, the STO substrate is immersed in Buffered Hydrofluoric acid (BHF) for 30 seconds and then immersed in DI water for 120 seconds again(**Fig. 2-1**). The STO substrate was then annealed in ambient atmosphere at 1000℃ for 3 hours[26]. This treatment has flattened the surface of the STO substrate. After treatment, the STO substrate shows a clean step-and-terrace surface(**Fig. 2-2**).

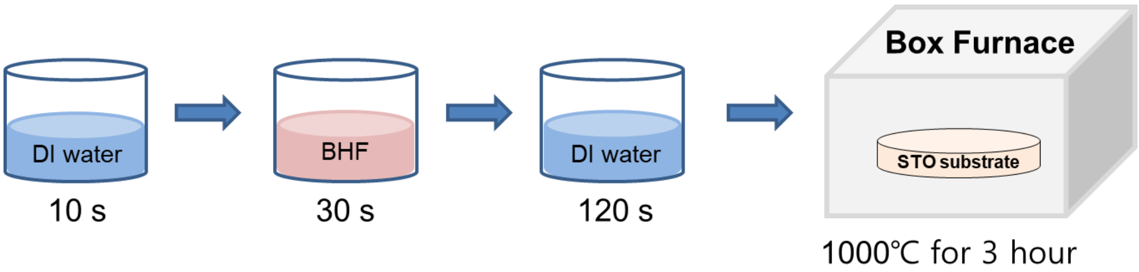

Fig. 2-1 The schematic of procedure of acid treatment.

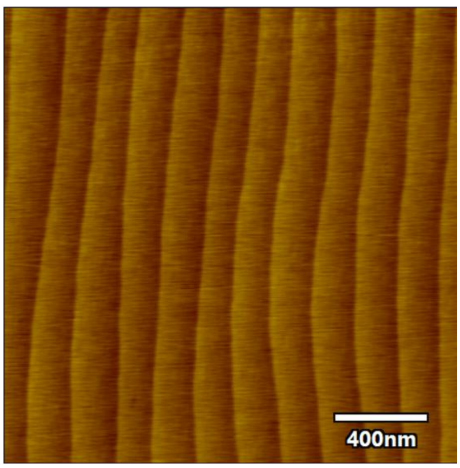

Fig. 2-2 AFM image of SrTiO3 substrate after acid treatment

SKBO thin films were grown using Pulsed Laser Deposition (PLD). **Fig. 2-3** shows a schematic of PLD system. The STO substrate was heated by laser diode heater. The KrF excimer laser enters the main chamber through the viewport and hits the target. The laser has a high energy, so it evaporates target when laser ablates target and as a result, plume is made. The plume approaches the STO substrate, and the films grows. SKBO has potassium (K) in A-site. K is volatile and could cause deficiency. To avoid this problem, it is common method to use a K over-doped target to compensate for possible K deficiency[16,17,20]. To grow the SKBO thin film, I used the $Sr_{0.4}K_{0.8}BiO_3$ target that was over-doped with K. Temperature, Oxygen pressure, and laser fluence are important parameters for film growth. The growth temperature changed from 600°C to 800°C. The oxygen pressure varied from 50 mtorr to 200 mtorr. The laser fluence changed from 0.5 J/cm^2 to 1.1 J/cm^2. The beam size of the KrF excimer laser was 1.8 x 1.2 mm^2, and the repetition rate was fixed at 3 Hz. After growing the SKBO thin film, I perform an *in-situ* post-annealing method to reduce oxygen vacancy. During the post-annealing method, the oxygen pressure is fixed at 400 torr. The temperature of the post-annealing varied from 600°C to 700°C and the time varied from 40 minutes to 160 minutes.

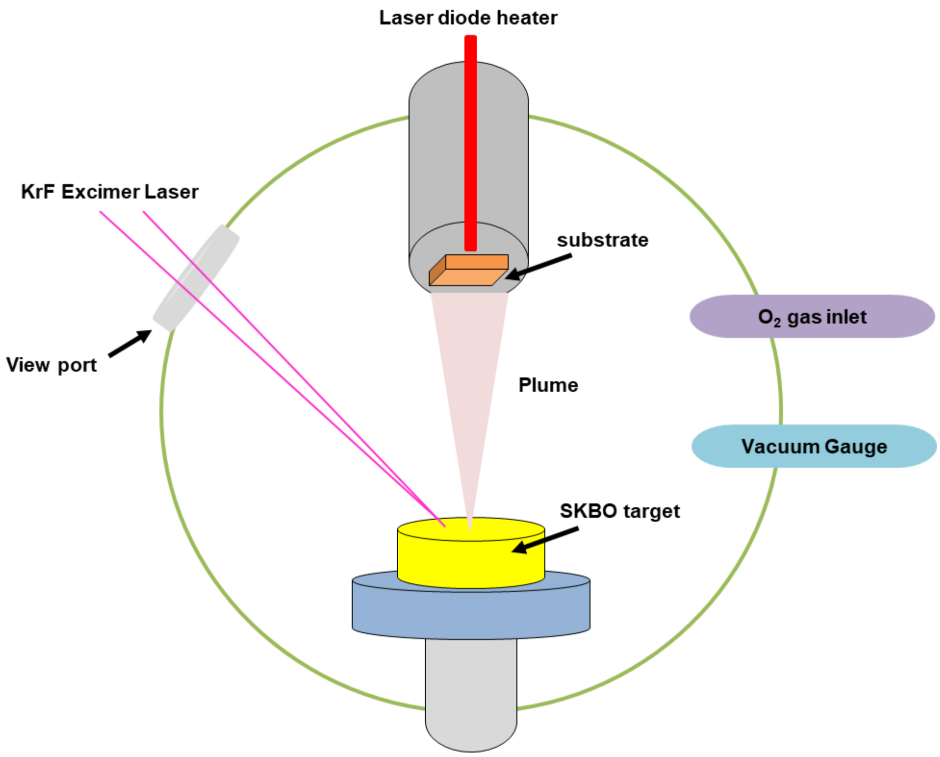

Fig. 2-3 The schematic of Pulsed Laser Deposition (PLD) system

2.2 Characterization of the thin film properties.

I used High-Resolution X-Ray Diffraction (XRD; Bruker, Germany). XRD is a powerful equipment that provides a lot of information about samples. The basic principle of XRD is Bragg's law. XRD uses Bragg's law to show information such as the lattice constant of the sample. XRD emits CuK-α X-ray (λ = 0.15406 nm) to the sample, and it diffracts the emitted X-ray. The detector absorbs the diffracted X-ray to show the data. By using XRD, I perform a 2θ-θ scan, Reciprocal Space Mapping (RSM) measurement, and X-ray Reflectivity (XRR) measurement. The 2θ-θ scan show the peaks of the substrate and the film. From the peak, the lattice constants for the substrate and the film could be calculated. In the RSM measurement, it is possible to see that the substrate and film (103) peak and to distinguish whether the film has grown epitaxially. XRR measurement was also performed. XRR is a useful method for determining the thickness of SKBO films.

I use ellipsometer (J. A. Woollam, USA) to see optical conductivity of the film. The ellipsometer uses light to determine the dielectric constant of the sample. The source emits linearly polarized light. This light is reflected by the sample, and the reflected light causes amplitude and phase changes. From this change, I can measure the optical properties of the sample. The ellipsometer shows the dielectric constant of the sample. The dielectric constant correlates with the light conductivity, so I can see the behavior of the light conductivity in the ellipsometer data. The film thickness is important in this experiment, so I check the film thickness before measuring the ellipsometer.

Physical Property Measurement System (PPMS; Quantum Design) is used to perform transport measurement. PPMS is a useful tool for identifying electrical properties. It uses liquid Helium, so it can cool down to 2 K. Therefore, I can see that the electrical properties of the samples change from low temperature to high temperature. A magnetic field could be applied to the sample to confirm the change in the electrical properties of the sample according to the external magnetic field. I measure the resistivity of the film at various temperature from 2 K to 300 K. I use the 4-probe method to check the resistivity of the film. Au 50 nm was deposited on the film using E-beam and Thermal Evaporator to create a 4-contact.

Chapter3

Results and Discussion

3.1 SKBO films growth without post-annealing method

I grew SKBO films on STO substrate without post-annealing method. The growth temperature was fixed at 700℃ and the oxygen pressure was fixed at 100 mtorr. Only the laser fluence changed from 0.4 J/cm^2 to 0.8 J/cm^2. After growth, XRD was used to determine how the SKBO film grew on the STO substrate. **Fig. 3-1** shows the results of a 2θ-θ scan of the SKBO film. **Fig. 3-1(a)** shows that there is only a substrate peak and no film peak According to Bragg's law, the peak of SKBO (002) is theoretically located at $2\theta \sim 42.8°$. There was a possibility that the XRD detector could not find the SKBO peak because it was too weak. So, I changed the scan range from 7° ~ 107° to 38° ~ 50° to reduce noise and accurately measure it. **Fig. 3-1(b)** shows the reduced scan range data. However, there was still no SKBO (002) peak. I assume that the volatility of potassium was so great that the peak of the SKBO film disappeared. So, I used capping layer to protect SKBO film.

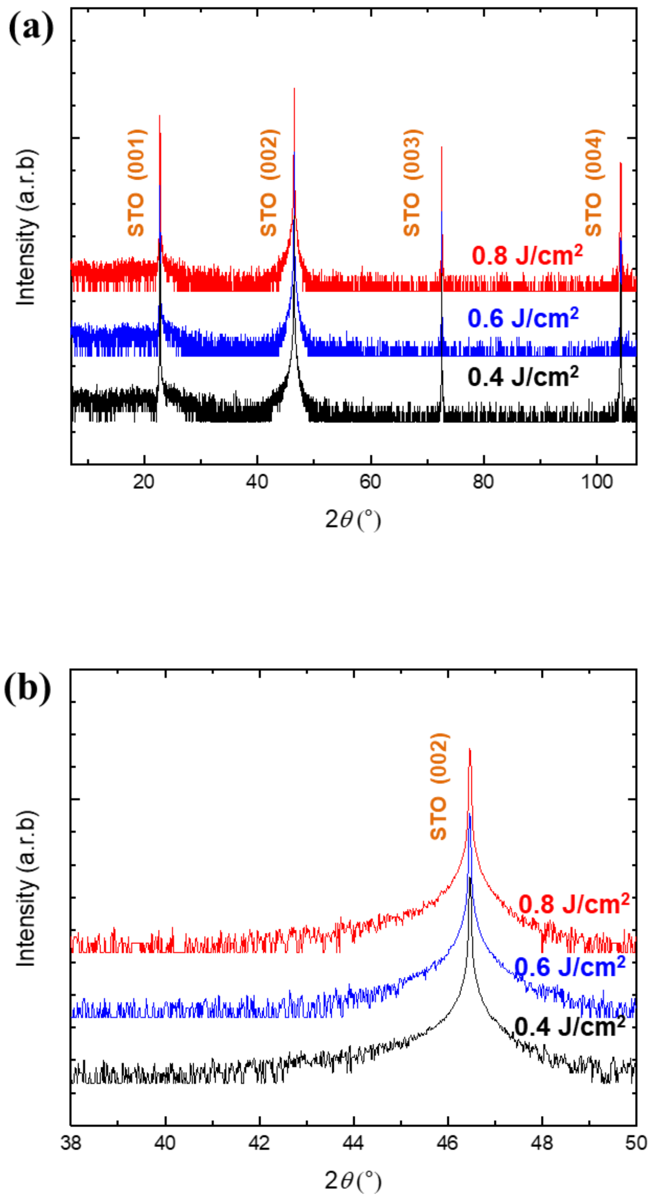

Fig. 3-1 X-ray Diffraction 2θ-θ scan without post-annealing method by varying laser fluence. The temperature and oxygen pressure are fixed at 700°C and 100 mtorr. The scan range is from (a) 7° to 107° and (b) 38° to 50°.

Using capping layer is a common way to protect films. I used the STO capping layer, which is the same as the substrate, to prevent the capping layer from being confused with the film peak. The STO capping layer grew 10 nm. This time, SKBO growth conditions were temperature 700℃, oxygen pressure 100 mtorr, and laser fluence 1.0 J/cm^2. The STO capping layer has a growth condition of temperature 700℃, oxygen pressurem100 mtorr, and laser fluence 1.0 J/cm^2. **Fig. 3-2** shows the XRD 2θ-θ results. The peak of the SKBO film appears. However, there are two big problems. The first is the disappearance of the peak. In **Fig. 3-2**, black line is the SKBO sample immediately after growth(As-growth) and red line is the same sample after 24 hours(24 h later). The peak of the SKBO film disappears after 24 hours. The second is the location of the peak. In **Fig. 3-2(b)**, the main (002) peak is located at $2\theta \sim 41°$. However, as mentioned earlier, the peak of SKBO (002) is theoretically located at $2\theta \sim 42.8°$. Therefore, I verify that the main peak in **Fig. 3-2(b)** is not the SKBO (002) peak. There was also a problem that SKBO samples could not be reproducible. The same growth conditions were used, but the same sample could not be grown. Based on these results, I came to think that it was not a volatile problem with potassium, but the oxygen vacancy problem. So, I need to find a way to reduce the oxygen vacancy.

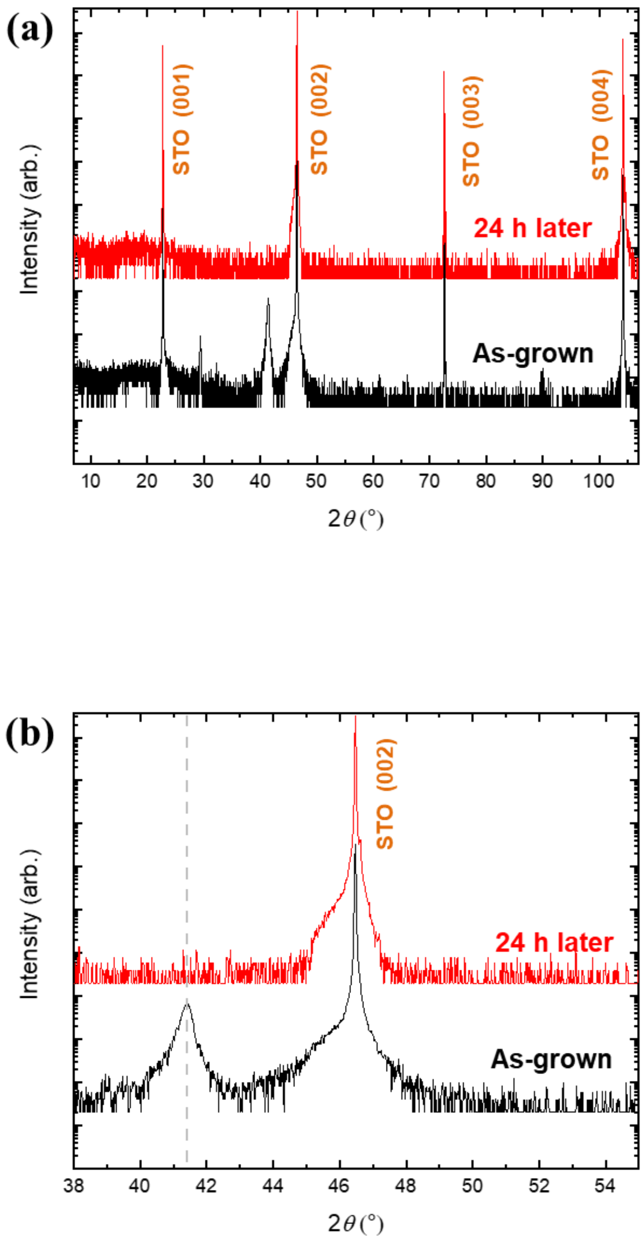

Fig. 3-2 X-ray Diffraction 2θ-θ scan with $SrTiO_3$ (STO) capping layer. The capping layer and film growth condition is that temperature, laser fluence and oxygen pressure are 700℃, 1.0 J/cm^2 and 100 mtorr. The black one is data immediately after growth (As-grown). The red one is data after 24 hours (24 h later). The scan range is from (a) 7° to 107° and (b) 38° to 55°.

3.2 SKBO films growth with post-annealing method

When the BKBO thin film was grown on the STO substrate, a post-annealing method was used to reduce oxygen vacancy[20]. Since SKBO is similar to BKBO, I expected that the oxygen vacancy of SKBO film would be reduced by using the same method. The post-annealing temperature was fixed at 700℃ and oxygen pressure was 400 torr to compensate the oxygen vacancy.

Before optimizing the growth conditions, I checked whether the post-annealing method actually worked. SKBO growth conditions were temperature 700℃, oxygen pressure 100 mtorr, laser fluence 1.0 J/cm^2. The post-annealing temperature and oxygen pressure were fixed at 700℃ and 400 torr. The SKBO film was in these condition for 40 minutes. **Fig. 3-3** shows the post-annealing results. **Fig. 3-3** shows that the peak does not disappear after 168 hours. Therefore, the post-annealing method is a useful tool to reduce the oxygen vacancy, and as a result, it is confirmed that the main peak does not disappear over time. In **Fig. 3-3**, I could see that there are additional peaks around $2\theta \sim 30°$. Therefore, it is necessary to find optimized growth conditions to eliminate additional peaks.

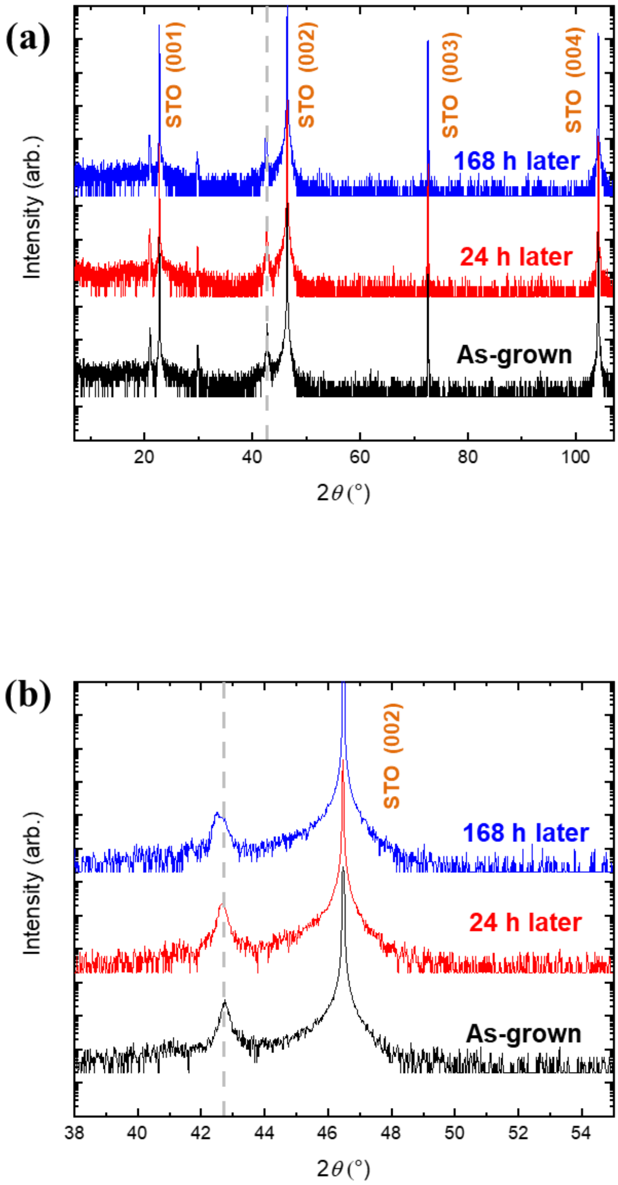

Fig. 3-3 X-ray Diffraction 2θ-θ scan with post-annealing method. The Temperature, laser fluence and oxygen pressure are 700°C, 1.0 J/cm^2 and 100 mtorr. The post annealing condition is that temperature is 700°C Oxygen pressure is 400 torr for 40 minutes. The black one is data immediately after growth (As-grown). The red one is data after 24 hours (24 h later). The blue one is data after 168 hours (168 h later). The scan range is from (a) 7° to 107° and (b) 15° to 55°.

First, the growth temperature was changed from 600℃ to 800℃. **Fig. 3-4** shows the results of a 2θ-θ scan of the SKBO film according to temperature changes with post-annealing. The main (002) peak is located at $2\theta \sim 42.78°$ **(Fig. 3-4)**. Theoretically, the SKBO film (002) peak is located at $2\theta \sim 42.8°$. Therefore, it is confirmed that the main peak is the SKBO (002) peak. However, there are additional peaks around $2\theta \sim 26°$, 31°, 51°. Since $2\theta \sim 26°$ is $(Sr,K)_5Bi_3O_{12}$ and $2\theta \sim 31°$, 51° are $(Sr,K)_3Bi_2O_7$ peaks [27,28]. So, SKBO film does not have a single phase under this condition.

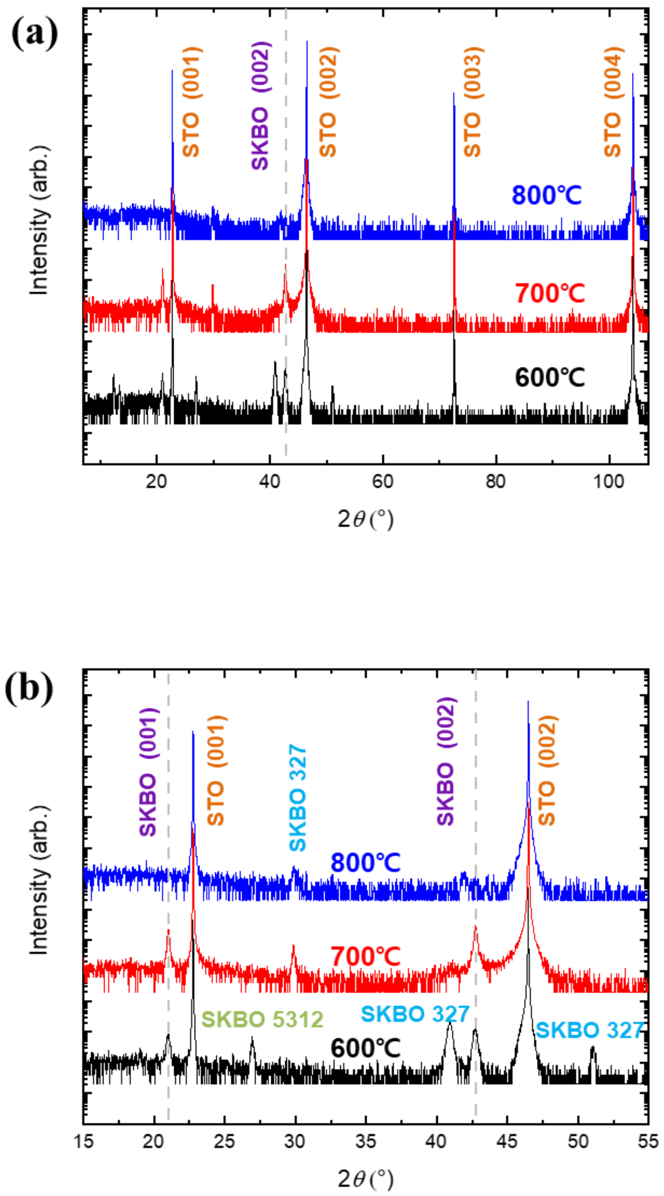

Fig. 3-4 X-ray Diffraction 2θ-θ scan with post-annealing method by varying temperature. The laser fluence and oxygen pressure are fixed at 1.1 J/cm^2 and 100 mtorr. The post annealing condition is that temperature is 700℃ Oxygen pressure is 400 torr for 40 minutes. The scan range is from (a) 7° to 107° and (b) 15° to 55°.

Second, I changed the laser fluence among the growth conditions. **Fig. 3-5** shows the results of the 2θ-θ scan of the SKBO film by changing the laser fluence with post-annealing. When the laser fluence is 1.1 J/cm^2, it is observed that an extra peak is present (**Fig. 3-5**). The peak is located at $2\theta \sim 51°$, but SKBO has no peak at $2\theta \sim 51°$. The peak located at $2\theta \sim 51°$ is $(Sr,K)_3Bi_2O_7$ peak[28]. Apart from the laser fluence 1.1 J/cm^2 XRD data, SKBO film shows that the lower the laser fluence, the weaker the SKBO (002) peak. Therefore, the optimized laser fluence is 0.9 J/cm^2.

(a)

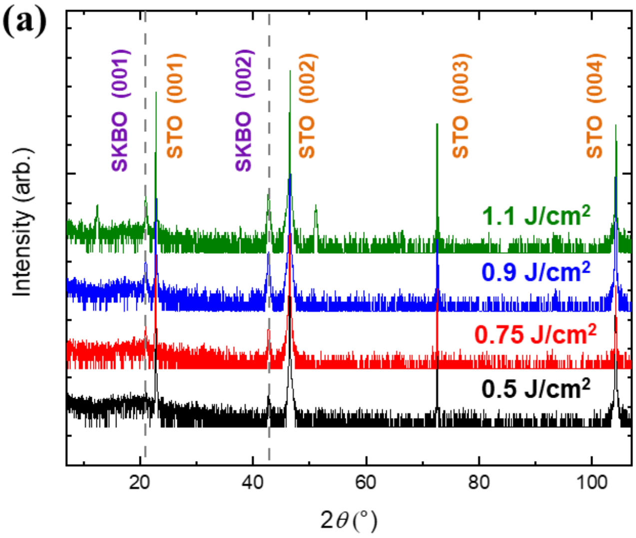

(b)

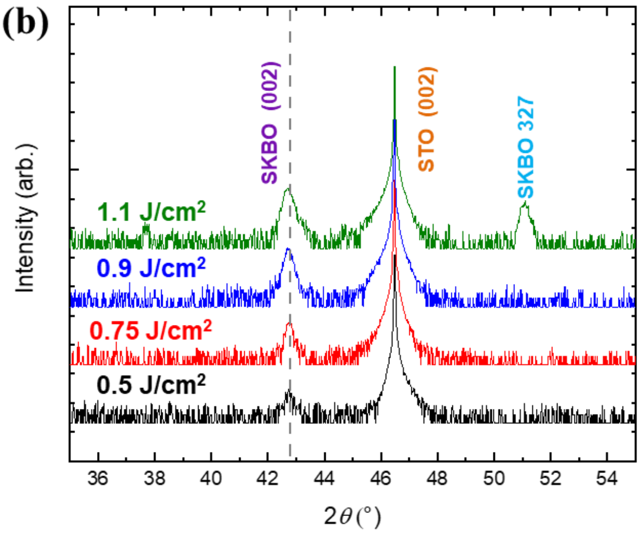

Fig. 3-5 X-ray Diffraction 2θ-θ scan with post-annealing method by varying laser fluence. The temperature and oxygen pressure are fixed at 700℃ and 100 mtorr. The post annealing condition is that temperature is 700℃ Oxygen pressure is 400 torr for 40 minutes. The scan range is from (a) 7° to 107° and (b) 38° to 55°.

The next step is to change the oxygen pressure. **Fig. 3-6** shows the results of a 2θ-θ scan of the SKBO film by varying the oxygen pressure with post-annealing. There is an additional peak around $2\theta \sim 51°$ at 50 mtorr, and at 200 mtorr, there is an additional peak around $2\theta \sim 41°$. As mentioned earlier, $2\theta \sim 51°$ and $2\theta \sim 41°$ are the $(Sr,K)_3Bi_2O_7$ peak[28]. Therefore, 100 mtorr oxygen pressure with no additional peak is the optimized growth condition.

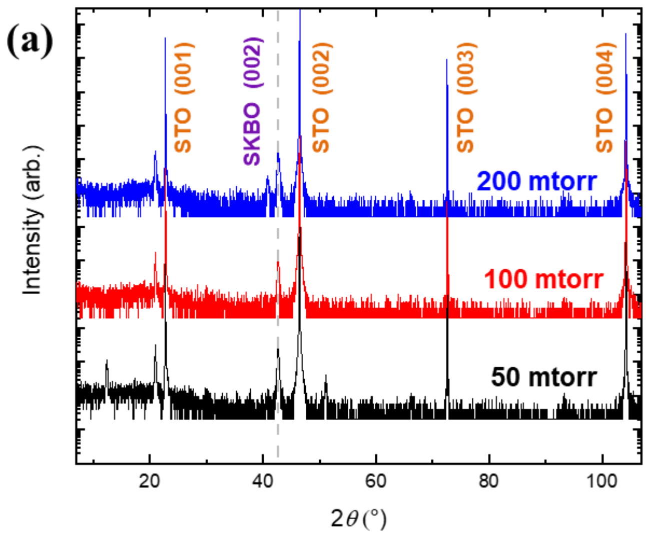

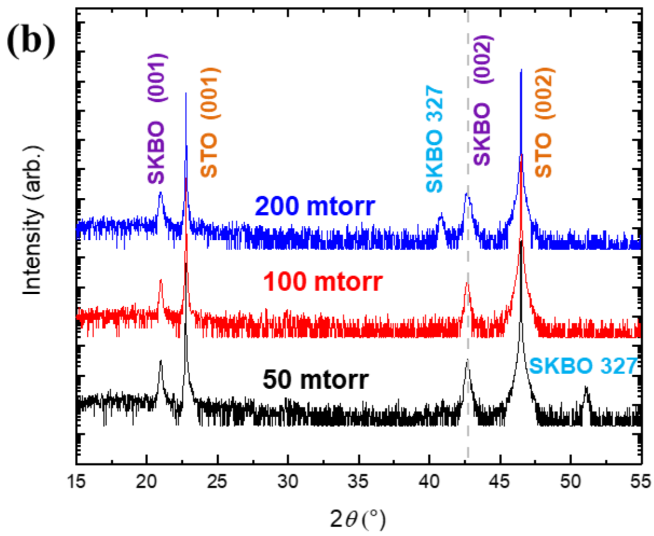

Fig. 3-6 X-ray Diffraction 2θ-θ scan with post-annealing method by varying oxygen pressure. The laser fluence and temperature are fixed at 0.9 J/cm^2 and 700°C. The post annealing condition is that temperature is 700°C Oxygen pressure is 400 torr for 40 minutes. The scan range is from (a) 7° to 107° and (b) 15° to 55°.

I confirmed that the optimized growth conditions found by changing the growth conditions were T = 700℃, oxygen pressure = 100 mtorr, laser fleuce = 0.9 J/cm^2. However, this is a condition for the film growth. I used a fixed post-annealing condition, so there is no information about the post-annealing condition. Therefore, I have grown new SKBO samples to find the optimized post-annealing condition(**Fig. 3-7**).

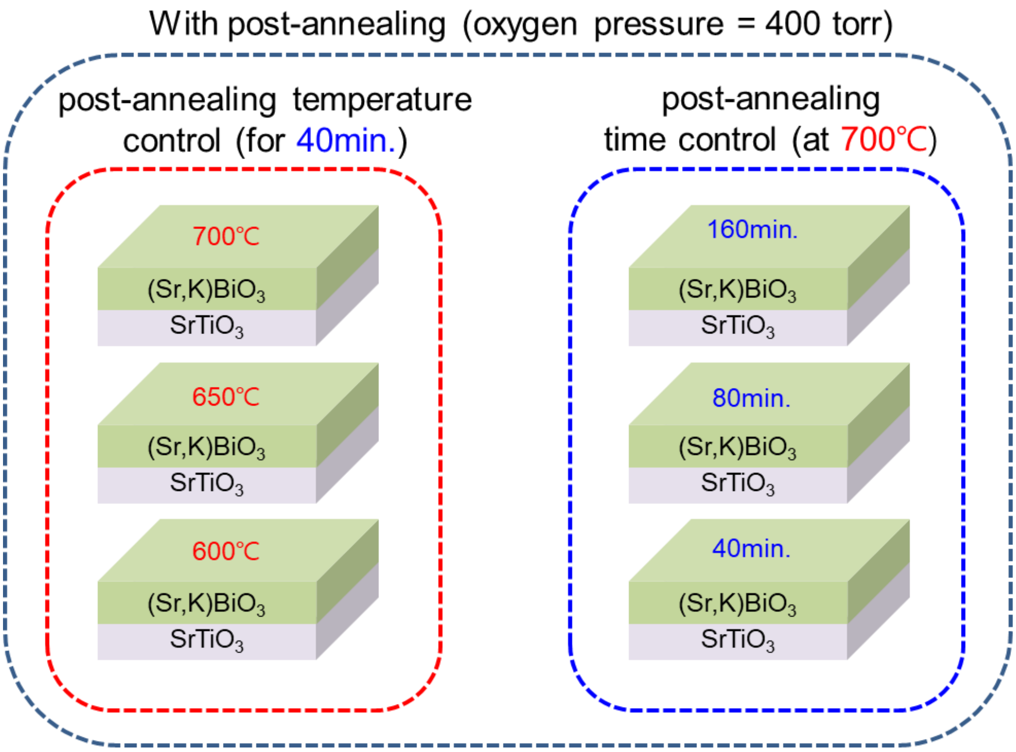

Fig. 3-7 The SKBO/STO samples. Post-annealing temperature and time are varied. Post-annealing oxygen pressure is fixed at 400 torr. All samples have the same films growth condition (T = 700°C, Oxygen pressure = 100 mtorr, Laser fluence = 0.9 J/cm^2).

First, I change the post-annealing time. **Fig. 3-8** shows the results of the 2θ-θ scan of SKBO films according to the post-annealing time. In **Fig. 3-8(b)**, there is an additional peak between 30° ~ 40°. These peaks are also $(Sr,K)_3Bi_2O_7$ peak[28]. Therefore, SKBO films have additional peaks after 40 minutes of post-annealing.

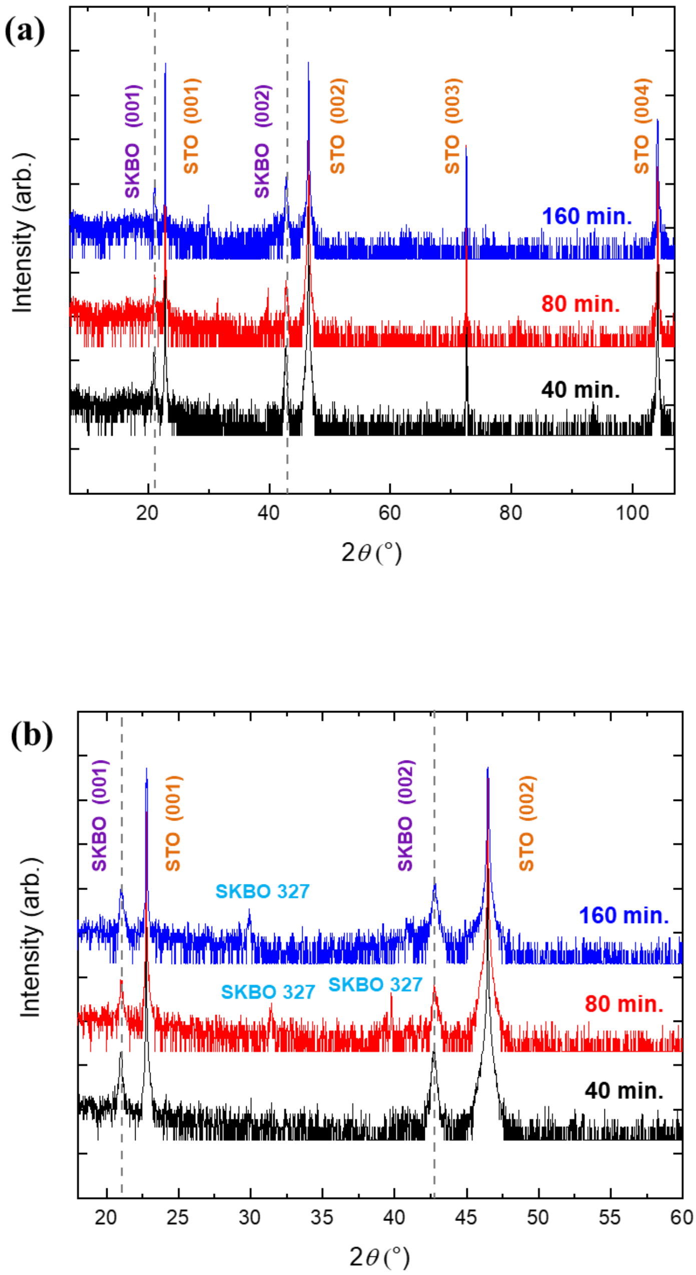

Fig. 3-8 X-ray Diffraction 2θ-θ scan of changing post-annealing time. The scan range is from (a) 7° to 107° and (b) 18° to 60°

Second, I change the post-annealing temperature. In BKBO films, the change in post-annealing temperature affects the electrical properties of the film, resulting in a change in the critical temperature[20]. Since SKBO is a similar material to BKBO, I expect it to affect the properties of the film. **Fig.3-9** shows the results of the 2θ-θ scan of the SKBO film according to the post-annealing temperature change. In **Fig. 3-9(b)**, there is an additional peak around the SKBO (002) peak. Unlike when the post-annealing time was changed, the additional peak exists between 40° and 50°. This peak corresponds to the $(Sr,K)_3Bi_2O_7$ peak[28], indicating that SKBO does not grow in a single phase on the STO substrate under the post-annealing temperature of T = 700℃. By changing the post-annealing condition, I verify that the optimized post-annealing condition is T = 700℃ and oxygen pressure = 400 torr for 40 minutes.

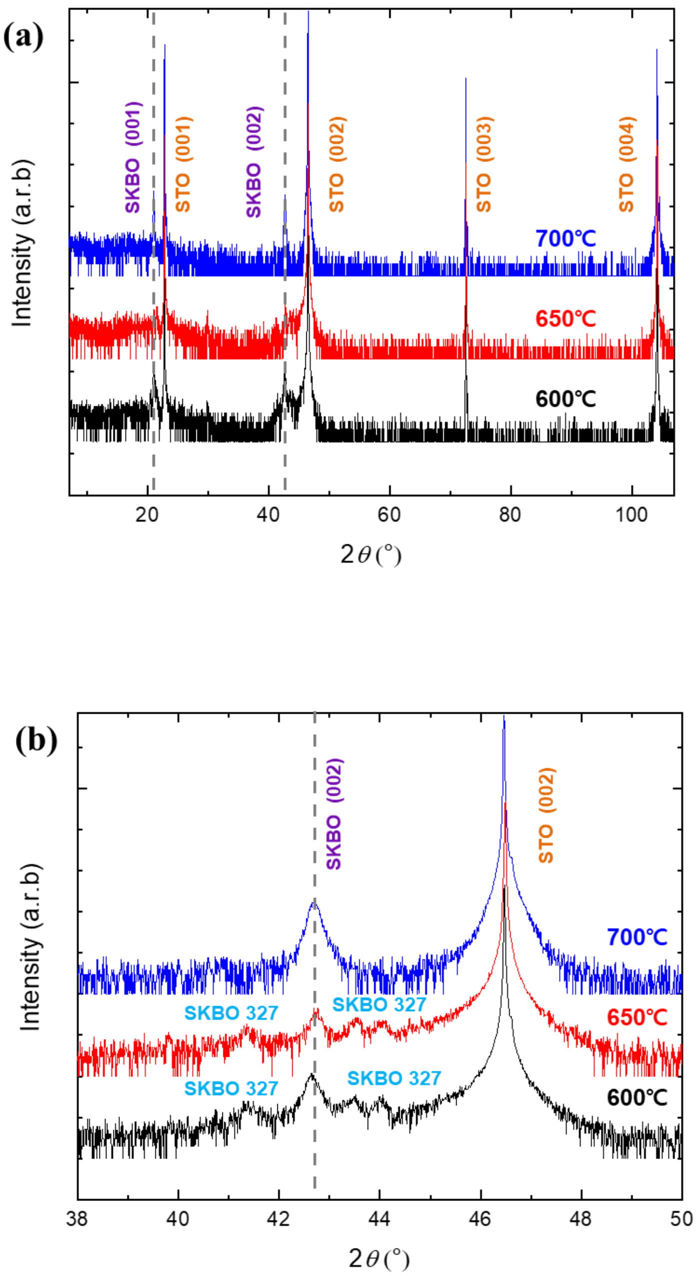

Fig. 3-9 X-ray Diffraction 2θ-θ scan of changing post-annealing temperature. The scan range is from (a) 7° to 107° and (b) 38° to 50°

The 2θ-θ scan shows that the SKBO film has a single phase on the STO substrate under optimized growth conditions. However, a 2θ-θ scan is not enough to confirm that SKBO film grows epitaxially on the STO substrate. Therefore, I performed a Reciprocal Space Mapping (RSM) measurement using XRD (**Fig. 3-10**). SKBO/STO samples grew under optimized growth conditions. **Fig. 3-10** shows only STO (103) and SKBO (103) peaks, no additional peaks found. Therefore, XRD 2θ-θ scan data and RSM measurements confirm that SKBO has grown epitaxially on the STO substrate under optimized growth conditions.

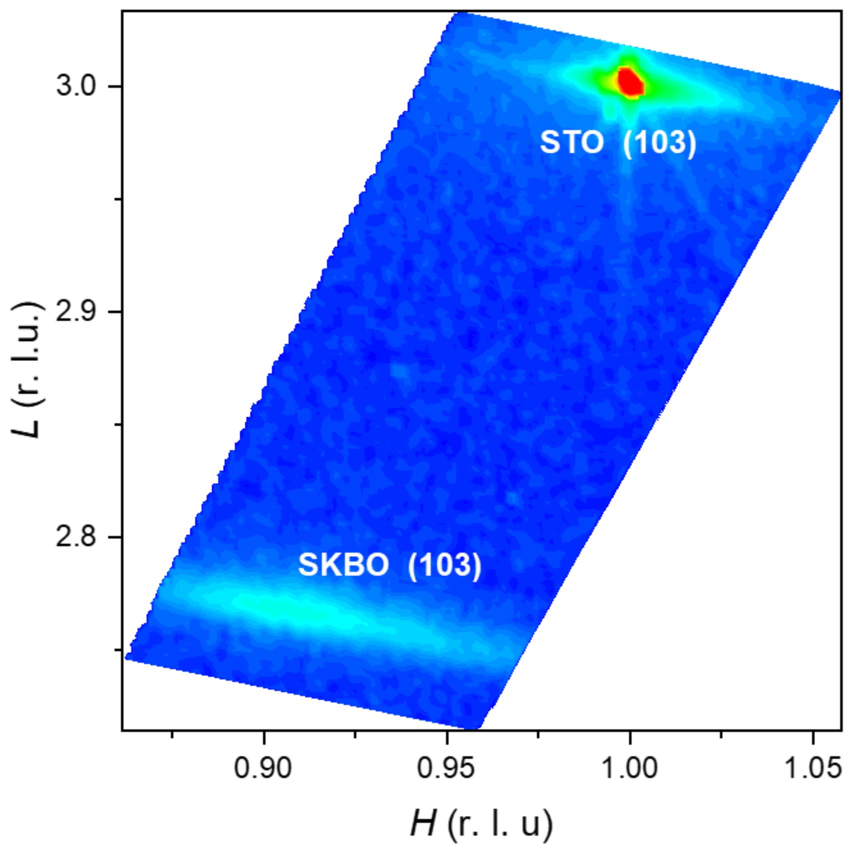

Fig. 3-10 The Reciprocal Space Mapping (RSM) around the STO (103) peak for a SKBO film. Film growth condition is that T = 700℃, Oxygen pressure = 100 mtorr and Laser fluence = 0.9 J/cm^2. Post-annealing condition is that T = 700℃, Oxygen pressure = 400 torr for 40 minutes.

3.3 Optical conductivity of SKBO films

I perform an ellipsometer measurement to see how the growth parameter affects the SKBO film. Through the measurement of the ellipsometer, I can know the dielectric constant of the sample. The tendency of optical conductivity can be determined through the dielectric constant because the dielectric constant is associated with optical conductivity. In here, I change laser fluence and post-annealing time.

Fig. 3-11 shows the change in the dielectric constant (ε_2) of the SKBO film when the laser fluence is varied. The change is particularly noticeable from 1 eV to 3 eV. There is no peak around 1 eV to 3 eV when the laser fluence is 0.5 J/cm^2. However, as the laser fluence increases, a peak appears. When the laser fluence is 1.1 J/cm^2, the peak is sharp and located at high position.

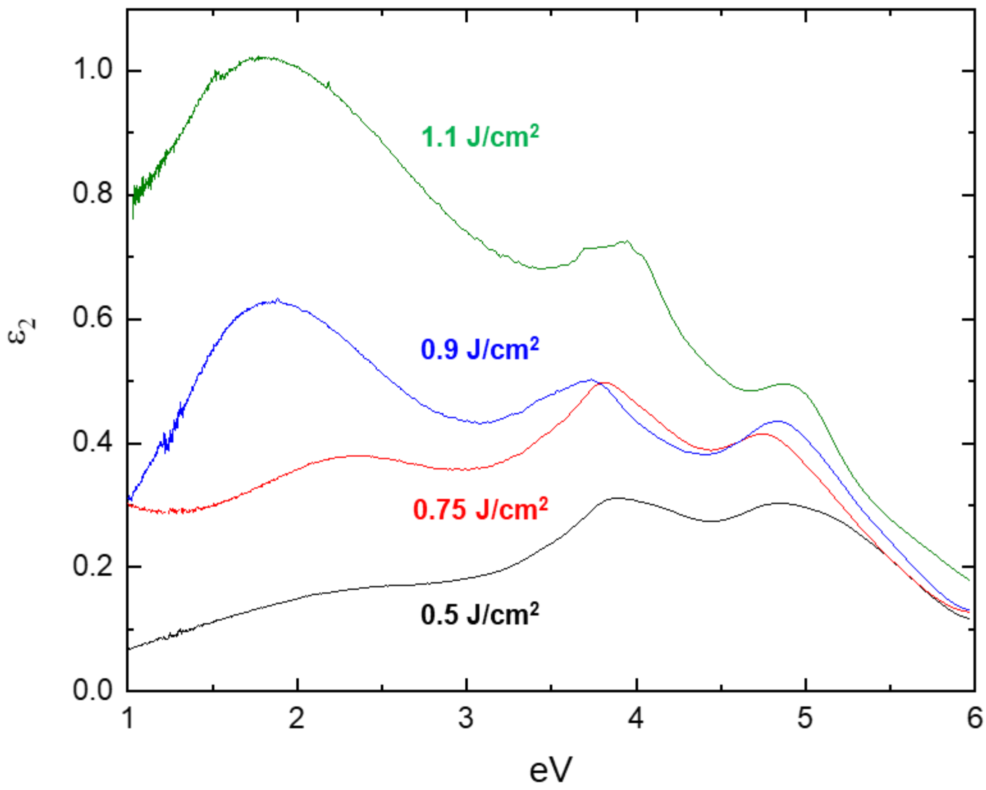

Fig. 3-11 Ellipsometer data of SKBO films. All samples have the same growth condition (optimized growth condition) except from laser fluence. The laser fluence is varied from 0.5 J/cm^2 to 1.1 J/cm^2.

Fig. 3-12 shows the dielectric constant (ε_2) of the SKBO film according to the post-annealing time. In **Fig. 3-12**, it can be seen that the post-annealing time affects the dielectric constant of the SKBO film. Changing the post-annealing time from 40 minutes to 80minutes increases the dielectric constant but changing the time from 80 minutes to 160 minutes decreases the dielectric constant and is placed below the 40 minutes sample.

The ellipsometer measurement confirmed that the laser fluence and post-annealing time affect the growth of SKBO films and make optical properties different.

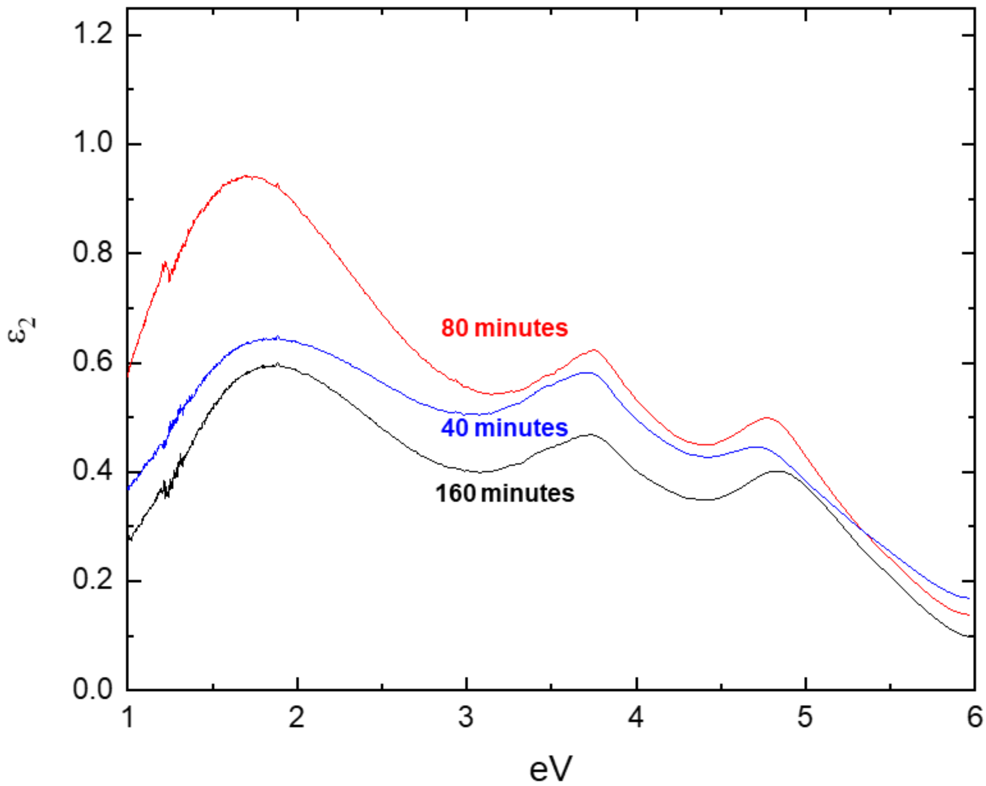

Fig. 3-12 Ellipsometer data of SKBO films. All samples have the same growth condition (optimized growth condition) except from post-annealing time. The post-annealing time is varied from 40 minutes to 160 minutes.

3.4 Electronic properties of SKBO films

I perform transport measurements of SKBO films (**Fig. 3-13(a)**). Since superconductivity has appeared in bulk SKBO, the SKBO film should have appeared the superconductivity. However, there is no superconducting phenomenon on the SKBO film. Under optimized growth conditions, the SKBO film shows only metallic behavior. In bulk state, $Sr_{1-x}K_xBiO_3$ shows superconductivity only when the potassium ratio x is in the range of 0.45 to 0.6. Therefore, I assume that the ratio of potassium is outside the range of superconductivity, so that SKBO films shows metallic behavior. The reason for this is that SKBO film growth used an over-doped potassium target with potassium ratio x of 0.8 to compensate for the K deficiency. However, during film growth, K in not deficient, and as a result, SKBO films are over doped with K. Since it is important to reduce the K ratio in the SKBO film, I tried to adjust the K ratio through laser fluence. In BKBO film, it is confirmed that the ratio of K varies through laser fluence[20]. Since SKBO is similar to BKBO, I assume that laser fluence could affect the K ratio of SKBO film. Therefore, transport measurements are performed with SKBO films that have changed the laser fluence. **Fig. 3-13(b)** is the transport measurement data obtained by changing the laser fluence. In **Fig. 3-13(b)**, the resistivity of the SKBO film increases as the laser fluence decreases. Therefore, I have confirmed that laser fluence affects the stoichiometry of SKBO films. However, there is still no superconductivity, only metallic behavior.

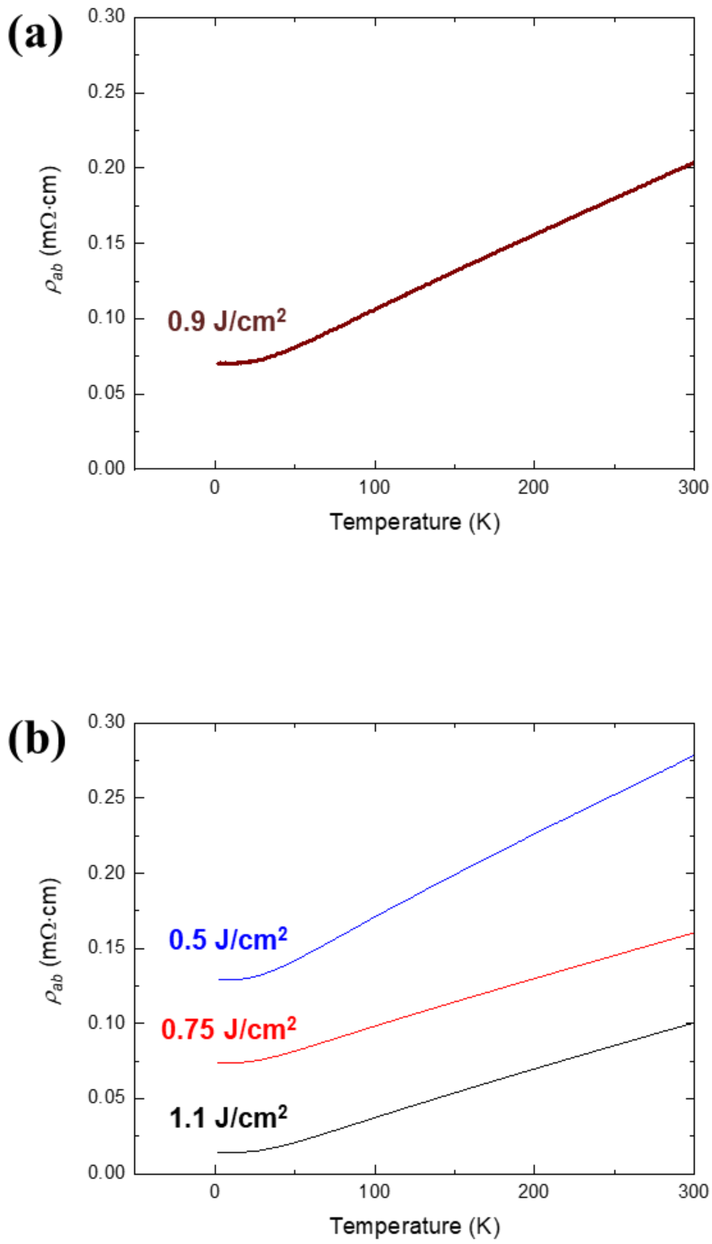

Fig. 3-13 The transport measurement data of SKBO film. The SKBO films are grown under optimized condition and only changes laser fluence. The laser fluence is (a) 0.9 J/cm^2 and (b) from 0.5 J/cm^2 to 1.1 J/cm^2.

Future Work

In this research, SKBO films show metallic behavior. Similar to BKBO, SKBO also affects the K ratio depending on the laser fluence. In fact, a decreasing in the laser fluence increases the resistivity, which could be attributed to the K ratio(**Fig. 3-13(b)**). However, all samples show metallic behavior. The BKBO film shows superconductor-to-insulator transition[20]. If the SKBO film shows superconducting behavior, the SKBO should show superconductor-to-insulator transition, just like BKBO. I want to lower the laser fluence to see the insulating behavior of the SKBO film at room temperature. However, SKBO films do not grow on the SKBO substrate under laser fluence 0.5 J/cm^2. It is concluded that it is difficult to grow a superconducting film using $Sr_{0.4}K_{0.8}BiO_3$ target. Therefore, I will use another target with a smaller K ratio. I will grow a new sample with a new target by change the laser fluence. I will perform transport measurement and Rutherford Backscattering Spectrometry (RBS) measurement. RBS is a useful tool for determining the composition of thin films. I could see the K ratio of samples growing under different growth conditions. As a result, I could control the K ratio on the SKBO films and adjust the K ratio to see the superconductivity on the SKBO film.

Conclusion

In summary, the SKBO thin film was grown on the STO substrate using Pulsed Laser Deposition. Initially, SKBO films grow on STO substrates without a post-annealing method. However, there were many problems, and the cause was determined to be oxygen vacancy. To solve this problem, I focused on the BKBO thin film. In the growth of BKBO thin films, post-annealing method is used to reduce oxygen vacancy. So, I used the same method. Using post-annealing method, SKBO films were grown well on STO substrate. XRD 2θ-θ data and RSM measurements confirmed that SKBO has a single phase when using the post-annealing method. By changing the growth conditions, I found the optimized growth conditions for SKBO film. While changing the post-annealing condition, it was confirmed that the post-annealing condition affects the SKBO film, and the optimized post-annealing condition was found. Ellipsometer and transport measurement were performed to investigate how growth and post-annealing condition affect the properties of SKBO films. In bulk state, SKBO shows superconductivity, and the critical temperature T_c is almost 12 K. At first, I expected SKBO films to show superconductivity. However, the experiment confirmed that the SKBO film showed metallic behavior. I thought that the reason for this tendency was that potassium was over-doped. So, I changed the laser fluence, and grew SKBO samples with different potassium ratio, and performed transport measurement again. Transport measurement data showed that the resistivity of the SKBO film increased when the laser fluence decreased. However, SKBO films still showed metallic behavior. In the future work, I will use less potassium doped target to grow SKBO films. Using less potassium doped target, I expect SKBO film to show superconductivity.

Reference

[1] N. Reyren, S. Thiel, A. D. Caviglia, L. F. Kourkoutis, G. Hammerl, C. Richter, C. W. Schneider, T. Kopp, A.-S. Rüetschi, D. Jaccard, M. Gabay, D. A. Muller, J.-M. Triscone, *and* J. Mannhart. *Superconducting Interfaces Between Insulating Oxides.* Science **317**, 1196 (2007)

[2] Fengmiao Li, Bruce A. Davidson, Ronny Sutarto, Hyungki Shin, Chong Liu, Ilya Elfimov, Kateryna Foyevtsova, Feizhou He, George A. Sawatzky, *and* Ke Zou. *Epitaxial growth of perovskite SrBiO3 film on SrTiO3 by oxide molecular beam epitaxy*. Phys. Rev. Materials **3**, 100802(R) (2019).

[3] A. Gozar, G. Logvenov, L. Fitting Kourkoutis, A. T. Bollinger, L. A. Giannuzzi, D. A. Muller, *and* I. Bozovic. *High-temperature interface superconductivity between metallic and insulating copper oxides.* Nature **445**, 782-785 (2008)

[4] A. Ohtomo, *and* H. Y. Hwang. *A high-mobility electron gas at the LaAlO3/SrTiO3 heterointerface*, Nature **427**, 423-426 (2004)

[5] Hosub Jin, Sonny H. Rhim, Jino Im, *and* Arthur J. Freeman. *Topological Oxide insulator Cubic Perovskite Structure.* Sci Rep **3**, 1651 (2013)

[6] Binghai Yan, Martin Jansen, *and* Claudia Felser. *A large-energy-gap topological insulator based on the superconductor* $BaBiO_3$. Nature Phys **9**, 709-711 (2013)

[7] Gang Li, Binghai Yan, Ronny Thomale, *and* Werner Hanke. *Topological nature and the multiple Dirac cones hidden in Bismuth high-*T_c *superconductors.* Sci Rep **5**, 10435 (2015)

[8] LingFei Wang, Qiyuan Feng, Yoonkoo kim, Rokyeon Kim, Ki Hoon Lee, Shawn D. Pollard, Yeong Jae Shin, Haibiao Zhou, Wei Peng, Daesu Lee, Wenjie Meng, Hyunsoo yang, Jung

Hoon Han, Miyoung Kim, Qingyou Lu, *and* Tae Won Noh. *Ferroelectrically tunable magnetic skymions in ultrathin oxide heterostructures*. Nature Mater **17**, 1087-1094 (2018)

[9] Masaki Uchida *and* Masachi Kawasaki. *Topological properties and functionalities in oxide thin films and interfaces.* J. Phys. D: Appl. Phys. **51**. 143001 (2018)

[10] H. Sato, S. Tajima, H. Takagi, *and* S. Uchida. *Optical study of the metal-insulator transition on* $Ba_{1-x}K_xBiO_3$ *thin films*. Nature **338**, 241 (1989).

[11] Taichiro Nishio, Javed Ahmad, *and* Hiromoto Uwe. *Spectroscopic Observation of Bipolaronic Point Defects in* $Ba_{1-x}K_xBiO_3$. Phys. Rev. Lett. **95**, 176403 (2005).

[12] Gideok Kim, Michael Neumann, Minu Kim, Manh Duc Le, Tae Dong Kang, *and* Tae Won Noh. *Suppression of Three-Dimensional Charge Density Wave Ordering via Thickness Control.* Phys. Rev. Lett. **115**, 226402 (2015).

[13] A. W. Sleigh, J. L. Gillson, *and* P. E. Bierstedt. *High-temperature superconductivity in the* $BaPb_{1-x}Bi_xO3$ *systems.* Solid State Commun. **17**, 27 (1975).

[14] R. J. Cava, B. Batlogg, J. J. Krajewski, R. Farrow, L. W. Rupp, Jr, A. E. White, K. Short, W. F. Peck, *and* T. Kometani. *Superconductivity near 30 K without copper: the* $Ba_{0.6}K_{0.4}BiO_3$ *perovskite.* Nature (London) **332**, 814 (1988).

[15] D. G. Hinks, B. Daborowski, J. D. Jorgensen, A. W. Mitchell, D. R. Richards, S. Pei, and D. Shi. *Synthesis, structure and superconductivity in the* $Ba_{1-x}K_xBiO_3$ *system.* Nature (London) **333**, 836 (1988).

[16] B. M. Moon, C. E. Platt, R. A. Schweinfurth, *and* D. J. Van Harlingen. *in situ pulsed laser deposition of superconducting* $Ba_{1-x}K_xBiO_3$ *thin films.* Appl. Phys. Lett. **59**, 1905-1907 (1991).

[17] Wei-Tai Lin, Shyi-Ming Pan, *and* Kouth Chen. *Oxygen partial pressure dependence of the in situ growth of $Ba_{1-x}K_xBiO_3$ films by laser ablation.* Jpn. J. Appl. Phys. **32**, 770 (1993)

[18] D.P. Norton, J. D. Budai, B. C. Chakoumakos, *and* R. Feenstra. *Epitaxial growth of $Ba_{1-x}K_xBiO_3$ thin films by pulsed-laser deposition.* Appl. Phys. Lett. **62**, 414 (1993)

[19] H. Sato, T. Ido, S. Uchida, S. Tajima, M. Yoshida, K. Tanabe, K. Tatsuhara, *and* N. Miura. *Superconducting and normal states of $Ba_{1-x}K_xBiO_3$ studied with use of high-quality thin films.* Phys. Rev. B **48**, 6617 (1993)

[20] Hodong Lee, Minu Kim, O. B. Korneta, Shinbuhm Lee, *and* Tae Won Noh. *Ablation laser fluence as an effective parameter to control superconductivity in $Ba_{1-x}K_xBiO_3$ films.* Curr. Appl. Phys. **17(5)**, 600-603 (2017)

[21] L. R. Gilbert, R. Messier *and* R. Roy. *Superconducting $BaPb_{1-x}Bi_xO_3$ ceramic films prepared by R. F. Sputtering.* Thin Solid Films **54**, 129 (1978).

[22] Minoru Suzuki, Youichi Enomoto, *and* Toshiaki Murakami. *Study on grain boundary Josephson junctions in $BaPb_{1-x}Bi_xO_3$ thin films.* J. Appl. Phys. **56**, 2083 (1984).

[23] Jinkwon Kim, Junsik Mun, Bongju Kim, Han Gyeol Lee, Daesu Lee, Tae Heon Kim, Shinbuhm Lee, Miyoung Kim, Seo Hyoug Chang, *and* Tae Won Noh. *Coherent-strained superconducting $BaPb_{1-x}Bi_xO_3$ thin films by interface engineering.* Phys. Rev. Mater. **11**, 113606 (2019)

[24] Kateryna Foyevtsova, Arash Khazrail, Ilya Elfimov, *and* George A. Sawatzky. *Hybridization effects and bond disproportionation in the bismuth perovskites.* Phys. Rev. B **91**, 121114(R) (2015)

[25] S. M. Kazakov, C. Chaillout, P. Bordet, J. J. Capponi, M. Nunez-Regueiro, A. Rysak, J. L. Tholence, P. G. Radaelli, S. N. Putilin *and* E. V. Antipov. *Discovery of a second family of bismuth-oxide-based superconductors.* Nature **390**, 148 (1997).

[26] Masashi Kawasaki, Kazuhiro Takahashi, Tatsuro Maeda, Ryuta Tsuchiya, Makoto Shinohara, Osamu Ishiyama, Takuzo Yonezawa, Mamoru Yoshimoto, *and* Hideomi Koinuma. *Atomic Control of the* $SrTiO_3$ *Crystal Surface.* Science ***266***, 1540 (1994)

[27] J. S. Pshirkov, S. M. Kazakov, A. M. Abakumov, S. N. Putilin, *and* E. V. Antipov. *Synthesis and Characterization of New Phase:* $Sr_{3.75}K_{1.75}Bi_3O_{12}$ *and* $Sr_{3.1}Na_{2.9}Bi_3O_{12}$. J. Solid State Chem., **152**, 492-502 (2000)

[28] J. S. Pshirkov, S. M. Kazakov, C. Bougerol-Chaillout, P. Bordet, J. J. Capponi, S. N. Putilin, *and* E. V. Antipov. *A New Layered Bismuthate* $(Sr, K)_3Bi_2O_7$*; Synthesis and Crytal Structure.* J. Solid State Chem., **144**, 405 (1999)

국문 초록 (Korean Abstract)

최근에 비스무스 산화물 박막에 관해서 많은 관심이 생겨났다[1]. 비스무스 산화물 얇은 박막 중에서 $BaBiO_3$ (BBO)의 물성을 조절하기 위해서 많은 연구들이 진행되었다. 그러나 BBO 와 유사한 성질을 지니고 있음에도 불구하고 $SrBiO_3$ (SBO)는 많은 관심을 받지 못하였다. SBO 를 박막으로 만든 연구는 2019 년에 분자선 결정 성장 시스템 (MBE)를 이용해서 박막으로 만든 것이 유일하다[2].

여기서 나는 SBO 에 칼륨을 넣은 $(Sr,K)BiO_3$ (SKBO) (T_c ~ 12 K) 박막을 길렀다. 나는 산소원자 결함을 제거하기 위해서 포스트 어닐링 방법을 사용하였다. 온도, 산소 압력, 레이저 세기를 변화시켜 가면서 SKBO 박막의 성질이 어떻게 달라지는지 확인해보았다. 게다가, 포스트 어닐링이 중요하다는 것을 보이기 위해서 포스트 어닐링 조건도 조절하였다. 엑스레이 회절, 타원계측법, 그리고 전기전도도 측정을 통해서 SKBO 박막의 특성을 관찰할 수 있었다. 이 연구를 통해서 새로운 종류의 비스무스 산화물 박막을 길렀다. 이를 통해서 비스무스 산화물 박막 연구를 할 수 있는 새로운 길을 제공한다.